UNITED NATIONS UNIVERSITY
UNU-GTP
Geothermal Training Programme

Orkustofnun, Grensasvegur 9,
IS-108 Reykjavik, Iceland

Reports 2018
Number 25

1D INVERSION OF MAGNETOTELLURIC DATA FROM MAINIT GEOTHERMAL AREA, PHILIPPINES

Jeffrey G. Sayco
Department of Energy, Energy Center
Rizal Drive Cor. 34th Street
Bonifacio Global City
Taguig City
PHILIPPINES
jgsayco@yahoo.com

ABSTRACT

Mainit geothermal project is one of the geothermal prospects located in Surigao del Norte, Philippines. Aside from hosting several warm springs, the province is also rich in minerals with abundant deposits of silver, copper, gold and nickel. Several studies have been conducted in the area to confirm the viability and feasibility of a geothermal system, the most recent one was undertaken in 2012 by Energy Development Corporation (EDC).

Magnetotelluric (MT) survey was conducted in 2012 to determine the subsurface resistivity structure of the area. Based on the result of the 1D inversion, three significant findings were observed: 1) A shallow, high-resistivity layer of the Paco-Maniayao Volcanic Complex (PMVC) is associated with the Young Paco-Maniayao volcanics; 2) A low-resistivity layer outcropping in the west and northwest of the PMVC is generally characterized by Tugunan sedimentary formations; and 3) A high-resistivity layer at depth, northeast of the area is believed to be an intrusive body which could be a heat source which is also responsible for the mineralization processes as manifested by mineral deposits. However, since the MT data were obtained close to the coast, the surrounding conductive sea makes interpretation difficult, especially the deep part of the subsurface which might give a different response in the inversion due to the effect of the sea.

1. INTRODUCTION

To fully understand a geothermal field, an effective geothermal exploration should be undertaken. Three main surveys should be conducted to better characterize the geothermal activity in an area: geological, geochemical and geophysical. Geological investigation deals with the study of the structure of the earth, which provides information on the volcanic history, ages of rocks and their type, and structures and geohydrology of the area. Geochemical surveying deals with the chemistry/analysis from water and gas samples of the underground reservoir fluid and steam in order to estimate the reservoir temperature. Geophysical exploration deals with the study of the physical properties in the subsurface through surface exploration techniques. The results are used to identify the flow of the fluid at the subsurface and estimate the shape and size of the geothermal reservoir.

The Philippines, as part of the Pacific Ring of Fire, host several low- to high-temperature geothermal fields. The country has been involved in the exploration, utilization and development of geothermal energy for more than 50 years. In 1967 the first geothermal power lit up an electric bulb in Tiwi, Albay. The country's installed capacity has now reached 1906 MWe making the country the third largest producer of geothermal energy after the United States and Indonesia. The Philippine Department of Energy continues to invest, explore and develop new geothermal areas for possible power generation and/or direct-use applications by awarding service contracts to geothermal developers through direct negotiations and/or an open and competitive selection process.

1.1 Project background

The Mainit geothermal project was awarded by the Philippine Department of Energy to Energy Development Corporation (EDC) on March 24, 2010 under the Geothermal Renewable Energy Service Contract (GRESC) No. 2010-03-021. It has an estimated total land area of 377 km^2, covering the municipalities of Mainit, Alegria, Tubod, Placer, Sison, Taganan and Surigao City in the Province of Surigao del Norte. Under the GRESC, EDC was given the privilege to explore and develop the geothermal area within the prescribed terms. Activities under these terms include the acquisition of permits and clearances, geoscientific works, drilling of exploratory wells, pre-feasibility studies and declaration of commerciality.

1.2 Location and accessibility

The Mainit geothermal project is situated in the northern end of Eastern Mindanao as shown in the small red box on Figure 1. The area is approximately 750 km southeast of the capital city, Manila. It occupies a major portion of Surigao del Norte province and is accessible by air or by sea. From Manila, daily domestic flights are available going to Butuan City and Surigao City with a flying time of approximately 60-90 minutes. Moreover, commercial sea transport is available from Manila en-route to Surigao City and Nasipit (west of Butuan City) ports with approximately 36-48 hours sea travel time. From both cities, all municipalities in the region can be accessed through the Pan-Philippine highway.

1.3 Exploration History

Several studies have been conducted in the Mainit geothermal area for possible power generation in the province of Surigao del Norte. These include geological mapping in 1975 and 1989, geochemical sampling in 1974-1989 and geophysical surveys in 1989.

In the mid-1970s, the Commission on Volcanology (COMVOL) first investigated the potential of thermal springs in Mainit and Placer, Surigao del Norte, for electric power generation. Results of the survey indicated the existence of an exploitable resource. Most hot springs were associated with major and secondary faults. Based on the presence of highly fractured rocks, it was concluded that a large geothermal reservoir might exist within the Mainit geothermal field. The result showed that the area was characterized by low-resistivity values (< 60 Ωm), indicating a geothermal reservoir in four localities, Barrio Silop, Masapilid dome, Brgy, and Kapayahan and Kinankaman (Panem, 1975).

In 1989, PNOC-EDC conducted a geoscientific investigation in the prospect. Results of the survey revealed the existence of a hot aquifer with estimated subsurface temperatures ranging from 189 to 211°C. However, the geothermal resource appeared to be relatively small and localized (Sanchez, 1989).

In 1989, further geophysical investigation was done and confirmed that the resistivity features within the prospect area are directly related to the underlying formational units. It was also confirmed that the shape of the low-resistivity anomaly did not show any distinct resistivity pattern associated with thermal

upflow and outflow phenomena (Catane et al., 1989). In the same year, PNOC-EDC conducted a follow-up integrated geoscientific survey in the area and the results indicate a small size geothermal system associated with unimpressive thermal manifestations and a carbonate rich reservoir. (Tebar and Pagado, 1990).

In 2012, Energy Development Corporation conducted an integrated resource assessment in the area, as part of their contractual obligation. The results showed that there is no mature geothermal system in the area and it is not favourable for conventional power generation.

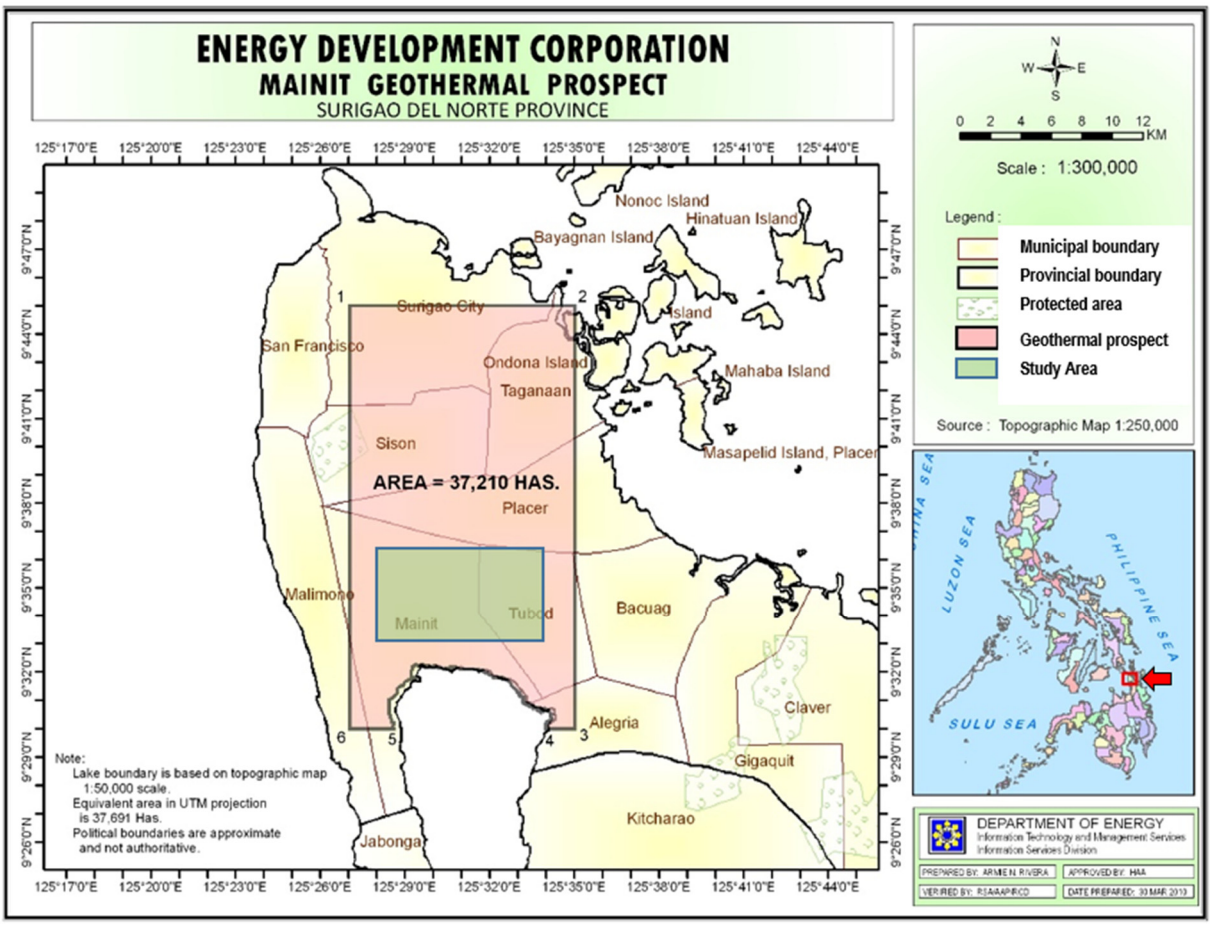

FIGURE 1: Geothermal service contract area of the Mainit geothermal project, showing the study area (DOE, 2010)

2. GEOPHYSICAL EXPLORATION

2.1 Overview

Geophysical surveys play an important role in geothermal exploration similarly to geological and geochemical investigations. The primary aim of the surveys is to delineate a geothermal resource, locate aquifers and identify the flow of fluids in the subsurface and estimate the shape and size of the geothermal reservoir. Unlike geological and geochemical surveys which are usually limited to direct observations on the surface, geophysical exploration deploys equipment in the field to measure some physical properties and parameters at depth. Physical properties that can be inferred include the sub-surface temperature, electrical resistivity, density, magnetization and seismic velocity.

An effective geophysical survey will provide an in-depth analysis and information about the geothermal reservoir. It also provides an input to a conceptual model of the area, a clue on the location of the best drilling target and contributes to a successful drilling program.

2.2 Methodology

There are several geophysical methods that are practiced in geothermal exploration all over the world. These include thermal, resistivity, gravity, magnetic and seismic methods. Each survey has a different approach and methodology depending on the nature of the field and the parameters one wishes to determine. The most widely used geophysical method in geothermal prospecting is the resistivity method, especially magnetotellurics (MT), which can measure the resistivity at great depths. Each method is briefly discussed here below.

2.2.1 Thermal method

The thermal method is a direct geophysical method that measures the subsurface temperature and heat. In geothermal systems, heat is generally exchanged through conduction and/or convection. In this method, temperature is measured in 20-200 m deep drill holes and an estimation of the temperature at depth is made from the temperature gradient (Hersir and Björnsson, 1991). Thermal images have been used to determine thermal characteristics of volcanoes, delineate thermal areas of steam and altered ground and hot spring activities, determine rock types and locate geologic faults and fractures.

2.2.2 Gravity method

FIGURE 2: Gravity measurements using a Scintrex (CG-5) gravimeter in the Mabini geothermal area, Philippines in 2014

Gravity is a passive method which measures the earth's gravitational field. The variations in gravity are due to lateral density changes of the subsurface rocks in the vicinity of the measuring point. Gravity methods are useful in detecting fault systems and intrusive bodies below the surface. Information on the fault system can be used to analyse and understand groundwater channels and water flow directions. At the same time, gravity data may be used to analyse volcanic rocks in the subsurface to aid in the location of the heat source. Gravity data are normally displayed on a contour map. The equipment used to measure the variations in the earth's gravitational field is a gravimeter, as shown on Figure 2. These are very sensitive mechanical instruments which measure the changes in the earth's gravitational acceleration (g) at one place relative to a fixed reference point (relative measurements). Several corrections are applied to raw gravity data collected in the field before they can be used for geological interpretation. The processing of measured gravity readings is known as 'gravity data reduction'. It is necessary to correct for the variations in gravity produced by sources which are not of direct geological interest. These include latitude, free-air, Bouguer, terrain, tidal and drift corrections. The final "corrected" values in a gravity anomaly constitute a Bouguer gravity map. A Bouguer anomaly is only due to lateral variations of density beneath the surface (Kearey et al., 2002).

2.2.3 Magnetic method

The magnetic method is a structural method that is used in geothermal exploration, often applied together with gravity in mapping geological structures. Detailed ground-magnetic surveys are used to identify concealed intrusive bodies, trace dykes, faults, buried lava and depth to the basement, and to locate hydrothermally-altered areas (Hersir and Björnsson, 1991)

2.2.4 Seismic method

Seismic methods map the seismic velocity of the subsurface. There are two main categories: active and passive seismic methods. In active seismic methods, an external source is used to artificially induce seismic signals, such as explosions, air guns, hammer devices or vibro trucks. The passive seismic method relies on natural earthquake sources. These help to map the location of the heat source, fracture density zones and to determine the fluid phase and reservoir size (Georgsson, 2013).

2.2.5 Resistivity method

Resistivity measurements are the most powerful geophysical prospecting method. They are used to delineate geothermal systems, locate aquifers and sometimes to estimate porosity and physical conditions within a geothermal system. Resistivity is directly related to the properties of interest, such as pore structure, amount of water (saturation), salinity of the water, steam content in the water, water-rock interaction (alteration minerals), temperature and pressure. The salinity of the water, temperature, porosity and water-rock interaction are of the greatest interest. The common principle of all resistivity sounding methods is to induce an electrical current in the earth and monitor signals generated by the current distribution, normally at the surface (Hersir and Björnsson, 1991).

The electrical resistivity of a material is defined as the electrical resistance (**Ω**) between opposite faces of a unit cube of a conductive material (Kearey et al., 2002). For a conductive cylinder, such as a rock material of resistance (R), length (L), and a cross-sectional area (A), its specific resistivity (ρ) is expressed by the equation:

$$\rho = \frac{RA}{L} \tag{1}$$

where ρ = Specific resistivity (**Ω**m);
R = Resistance (**Ω**);
A = Area (m^2);
L = Length (m).

Geothermal water reacts with rocks to form secondary alteration minerals. Alteration starts just below 100°C where low-temperature zeolites and clay minerals, normally smectite, are formed. This zone is usually called the smectite-zeolite zone as shown in Figure 3. At the temperature range from 230 to 250°C, the low-temperature zeolites disappear and the smectite is transformed into chlorite. At temperatures above 250 °C, chlorite becomes the dominant alteration mineral. At higher temperatures epidote is formed (Árnason et al., 2000).

Resistivity methods in geophysical exploration can be divided into two categories: DC and AC methods. In DC-resistivity methods a constant current is introduced into the ground through a pair of electrodes at the surface which creates a potential field in the earth. By measuring the electric field (potential difference over a short interval), the subsurface resistivity can be inferred. The most widely used method is the Schlumberger method. The limitations of the DC-methods include a relatively slow progress in the field and limited depth of penetration (Hersir and Björnsson, 1991).

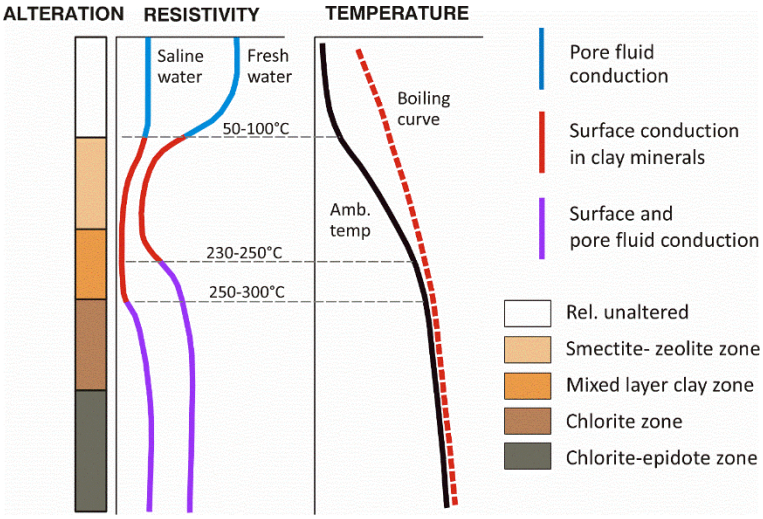

FIGURE 3: Resistivity of rocks and its relation to alteration and temperature (Flóvenz et al., 2012, modified from Flóvenz et al., 2005)

In AC-resistivity methods, an alternating current is induced in the earth. The alternating current may be a natural signal or artificially induced AC. Resistivity methods may further be classified as frequency domain or time domain. Magnetotelluric (MT), controlled source magnetotelluric (CSMT) and audio magnetotelluric (AMT) are frequency domain methods. In the frequency domain methods, measurements are made at different frequencies. Higher frequencies are attenuated faster than low frequency waves that penetrate deeper and therefore, high frequencies image the shallower part and lower frequencies the deeper part of the subsurface. In the time domain method, current is transmitted in a loop of wire and the decay of the induced magnetic field is measured as a function of time. The Transient electromagnetic method (TEM) is an example of this method (Hersir and Björnsson, 1991).

3. MAGNETOTELLURIC (MT) SURVEY

3.1 MT Basic Concept

Magnetotelluric (MT) is a passive electromagnetic (EM) technique that measures naturally occurring time-varying magnetic and electric fields at the surface of the earth in order to determine the resistivity of the subsurface. The method makes use of the response of the ground to the propagation of the electromagnetic waves. The response is dependent on the characteristics of rocks and minerals below the surface. By measuring the fluctuating magnetic field and electrical field in orthogonal directions on the surface of the earth, it is possible to infer the subsurface resistivity (Hersir and Björnsson, 1991).

The MT signals, as shown in Figure 4, can be divided into two parts: the low-frequency signal (<1 Hz) and the high-frequency signal (>1 Hz). The low-frequency signal originates from the magnetosphere and the interaction of the solar wind with the earth's magnetic field. The high-frequency signal is created by worldwide thunderstorm activity, usually near the equator, which is distributed as guided waves between the ionosphere and the earth to higher latitudes (Christopherson, 1998).

The governing equations that dictate the behaviour of electric and magnetic fields and their interdependence are the Maxwell equations. These equations are based on Faraday's and Ampere's laws, and are given by:

Faraday's law

$$\nabla \times \boldsymbol{E} = -\mu \frac{\partial \boldsymbol{H}}{\partial t} \tag{2}$$

Ampere's law

$$\nabla \times \boldsymbol{H} = \boldsymbol{J} + \varepsilon \frac{\partial \boldsymbol{E}}{\partial t} \tag{3}$$

where $\boldsymbol{E}$ = Electrical field intensity (V/m);
$\boldsymbol{H}$ = Magnetic field intensity (A/m);
$\boldsymbol{J}$ = Electrical current density, and $\boldsymbol{J} = \sigma \boldsymbol{E}$;

σ = Conductivity (Siemens/m); $\rho = 1/\sigma$ (Ωm);
ε = Electric permittivity;
μ = Magnetic permeability.

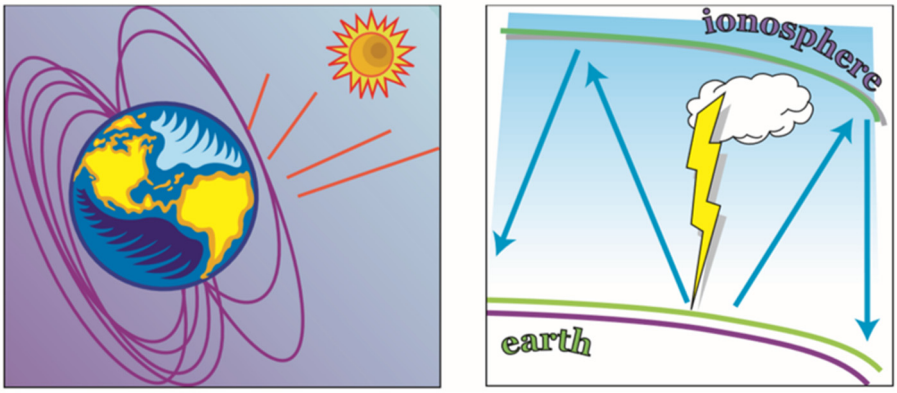

FIGURE 4: MT signals caused by low frequency *(left)* and high frequency *(right)* (adapted from Christopherson, 1998)

In a one-dimensional (1D) earth, the resistivity structure varies only with depth but not in horizontal directions. The fluctuating magnetic field (**H**), propagates vertically downwards below the earth's surface inducing an electric field (**E**) in the subsurface. Their relationship at each frequency involves a characteristic impedance tensor (**Z**), given by $\boldsymbol{E} = [\,\boldsymbol{Z}\,]\,\boldsymbol{H}$ (Hermance, 1973). No electric field is induced parallel to the induced field thus $Z_{xx} = 0$ and $Z_{yy} = 0$. In addition, the off-diagonal elements are non-zero but are equal in magnitude with opposite signs $Z_{yx} = -Z_{xy}$. The characteristics impedance, **Z** for a 1D earth is then given by (Vozoff, 1990):

$$\begin{bmatrix} E_x \\ E_y \end{bmatrix} = \begin{bmatrix} 0 & Z \\ -Z & 0 \end{bmatrix} \begin{bmatrix} H_x \\ H_y \end{bmatrix} \tag{4}$$

In MT, the data suffer from the so called telluric or static shift problem. Static shift is a phenomenon either caused by a shallow local conductivity anomaly or by current distortion due to topography. The shift is due to accumulation of charges at discontinuities, resistivity boundaries, near-surface resistivity inhomogeneities or topographical variations. It comes from the scaling of the apparent resistivity by a constant factor, in log scale (Jones, 1988). This phenomenon must be taken into consideration as it can lead to a large error in the inverted data. Several methods have been used to correct for static shift and the most widely used method is by conducting TEM survey in the same location and jointly invert the co-located MT and TEM data, since TEM measurements do not suffer from the static shift problem. However, in this particular survey conducted by EDC in 2012, no TEM survey was conducted. On the other hand, static shift corrections were taken into account by EDC during the 2D inversion process using the WinGlink software wherein the software has an option to invert for static shift. The algorithm simply states that the product of the shifts for one profile is equal to one (Africa, 2018)

3.2 Data acquisition

3.2.1 Equipment calibration

To ensure that all equipment was working well, EDC conducted a full calibration of all the sensors and receivers before the survey began. The results and graphs met all the requirements; the graphical results are the same for all the instruments. Figure 5 shows the calibration responses of the MTU2777 receiver and COIL6003 sensor.

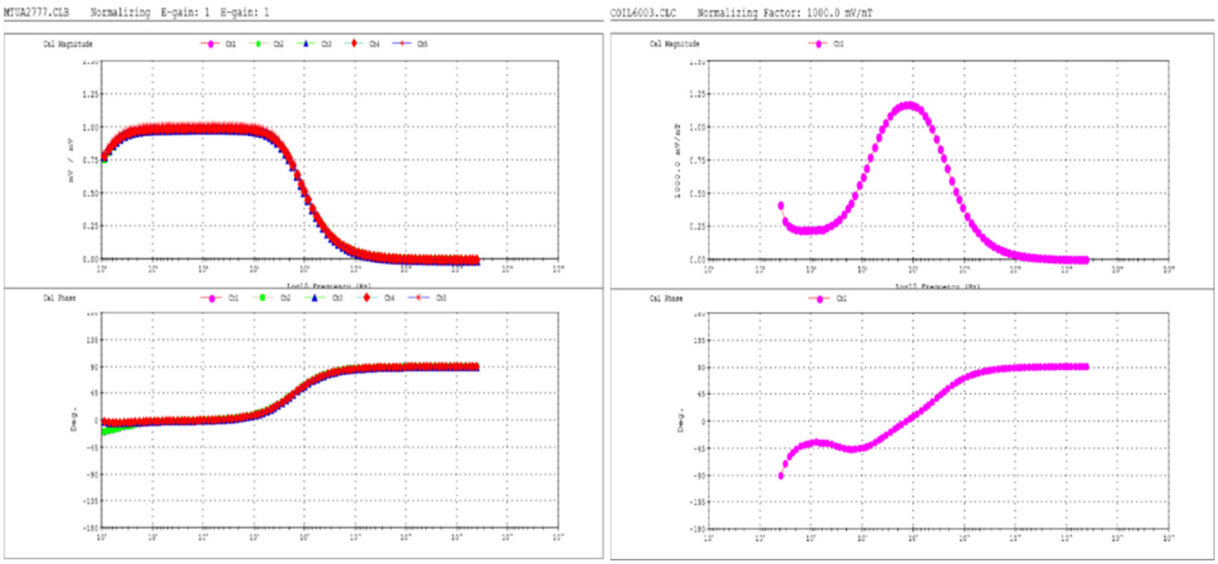

FIGURE 5: Calibration response of MTU2777 receiver (left) and COIL6003 sensor (right)

3.2.2 MT measurements

MT measurements in the Mainit prospect area were performed by Energy Development Corporation (EDC) from June 25 to September 25, 2012. A total of 96 sites were recorded in a grid pattern with a station spacing of about 600-1000 m depending on the terrain. MT stations were located in plain to gently sloping terrain. These stations were reached by riding a 4x4 wheel vehicle or by trekking.

Acquisition of MT data was done using MT equipment from Phoenix Ltd in Canada (MTU type) consisting of a data logger, three induction coil magnetometers, four E-field probes, cable wires, GPS antenna and a 12 V battery. Phoenix Geophysics MT equipment can be operated as a standalone system, in a network or as part of an array in which each unit is synchronized by its built-in GPS clock. It is housed in a small waterproof box, about 8 kg in weight. It comprises the complete circuitry for analogue signal conditioning, 24 Bit A/D conversion and data storage. A very precise GPS-controlled time base guarantees synchronous recordings even under difficult GPS reception conditions. Local labourers were hired to carry all the equipment and serve as guides to locate the proposed MT stations. In the MT survey, three sets of Phoenix instruments were used: One unit served as a base station for remote referencing while the remaining two served as roving units and were operated in the exploration area.

The survey employed a pull out-set up scheme wherein the crew proceeded toward the next station after downloading and an initial checking of data recorded during the previous night. At the designated roving station (see Figure 6), five measurements are recorded. They are the magnetic field (applying magnetic coils) in two horizontal directions (H_x and H_y) and one vertical direction (H_z), and the electric field (telluric pots) in two horizontal directions which are laid out in N-S (E_x) and E-W (E_y) directions, approximately 20-50 m apart depending on the condition, slope of the ground and presence of obstructions such as trees or roots. These pots are buried a few tens of centimetres in the ground. The electric and magnetic field sensors are connected to the MTU-5A receiver, which is placed at the centre of the field set-up. The magnetic sensors are laid next in between telluric lines. The north horizontal coil is laid in the northeast quadrant with its head pointing to the north while the east horizontal coil is laid in the southeast quadrant with its head pointing to the east direction. The vertical coil is placed in the southwest quadrant in hole that's more than 1 m deep. The horizontal magnetic coils are levelled horizontally using a bubble level and buried in 25 cm deep holes. Both the telluric and magnetic lines are colour-coded or knot-tied to monitor problematic pots, cable misconnection and polarity error. After the lay-out, measurement of contact resistance and local noise follows using the tester and a digital multimeter. These values are then logged and recorded in the toughbook computer. The MTU-5A unit

is then connected to two 12 V batteries. Power is switched on and a checking of the sensor signal follows. The clock is then GPS synchronized using a GPS antenna. After synchronization, gain setting for high, medium and low frequencies follows and the equipment is now preset for overnight measurement.

The actual location of the MT stations was determined by GPS and were subsequently plotted. Pertinent data such as coordinates, elevation, location, serial numbers, gain settings, azimuth, weather condition, and field description were noted and recorded in the MT data sheet and laptop computers.

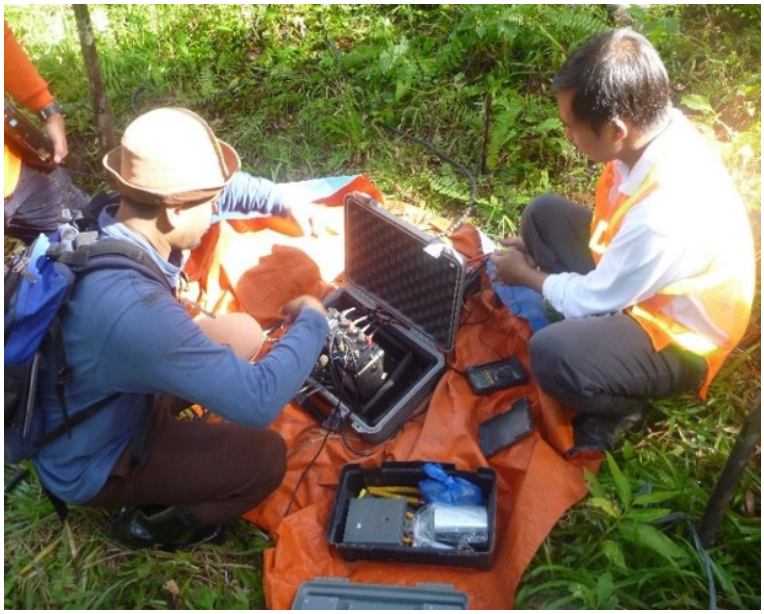

FIGURE 6: MT data acquisition in Mainit geothermal area using Phoenix MT instruments (09 July, 2012)

Data acquisition is done on a 20-40 hours synchronization to ensure good quality MT data. Data quality control is carried out routinely on site by operators before and during the measurements to catch errors and to ensure that correct field procedures are followed and the data are within its prescribed specifications. Data are downloaded and reviewed on-site to ensure that good quality data are obtained during the overnight measurements. The station resistivity and phase were plotted side by side according to station location to establish curve trend and similarities.

3.2.3 Remote reference

The remote reference method involves deploying an MT station at a remote, electronically quiet site and to correlate the remote data with data from the local measurement site, recorded at exactly the same time. This was implemented during the course of the survey to remove coherent magnetic noise in roving stations such as those caused by power lines, lightning and other cultural noises (Christopherson, 1998).

In this survey, the roving MT receiver collects data at different sites located within the project area while another MT receiver records data at a fixed remote site which was stationed within Jabonga, Agusan Del Norte which is about 30 km south of the survey area (see Figure 7).

3.3 Data processing

Data processing is accomplished using the Phoenix software modules: SSMT2000 and MTEditor. The SSMT2000 software was used to view and download the time series and calibration files, edit .tbl files and create output .mtl and .mth files. These output files were then used to generate an .edi file using the MTEditor.

After data acquisition, raw MT data, which are finite time series, were checked. The time series from a roving site and a remote site were Fourier transformed and their two, independent cross-powers were calculated. The resulting xy and yx resistivities were edited through automatic or manual editing and converted to a more generic and standard file structure called the *electronic data interchange* (.edi) format. In this case, several processing techniques were applied to obtain better resistivity and phase curves. Generally, remote referencing is very helpful to minimize local noise caused by power lines,

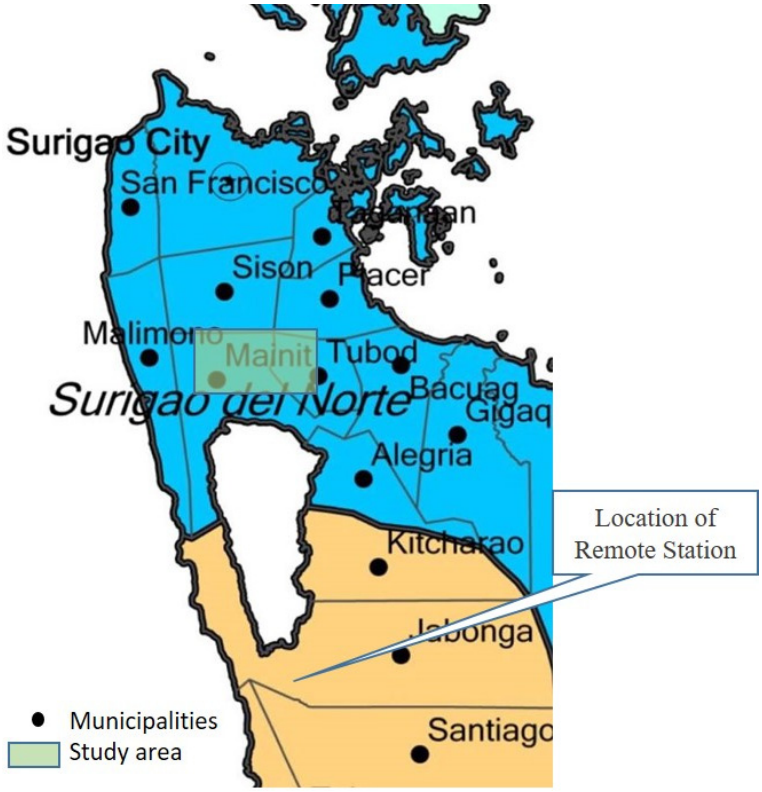

FIGURE 7: Location of remote reference station (adapted from Wikipedia, 2018)

lightning and other cultural sources. This can be seen in Figure 8, where the noise is minimized from 1 to 0.1 Hz using the remote reference technique for station MNT-020.

Two schemes of initial processing that attempt to filter out noise-affected data are controlled by the robust processing parameters: coherency and ρ-variance. This process reduces the size of the error bars and smooths the apparent resistivity curve. In this case, a weight is calculated from the local-remote magnetic coherency and used to reject up to 35% of the data to attempt to reach a coherency of 0.85. In the second phase, a ρ-variance scheme is used to reject up to 25% of the remaining data in attempting to reach a variance of 0.75 (Phoenix Geophysics, 2005).

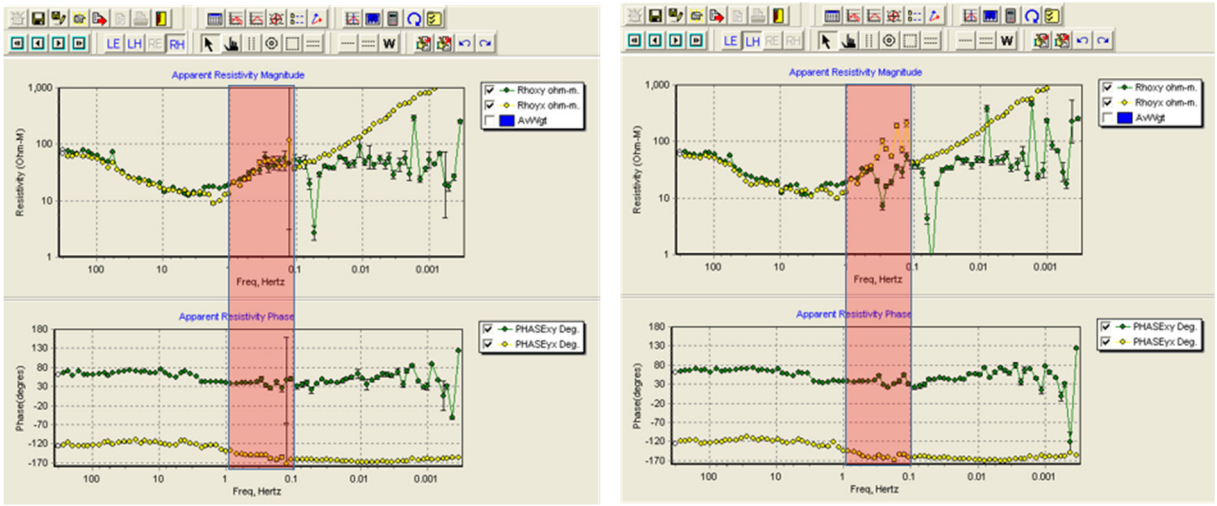

FIGURE 8: Comparison between using remote reference station (left) and without remote reference (right) at station MNT-020

In Figure 9, a comparison between the robust and non-robust processing is shown for station MNT-008. There, two slightly different curves are generated, particularly at 1-0.1 Hz. Theoretically, what a robust processing algorithm does is to compute the transfer functions but not allowing a few outliers to dominate the estimate (Pinto et al., 2011). For station MNT-008, the non-robust processing was used since it gave a better and more realistic result. Resulting EDI files from the processing can be seen in Appendix I (Sayco, 2018).

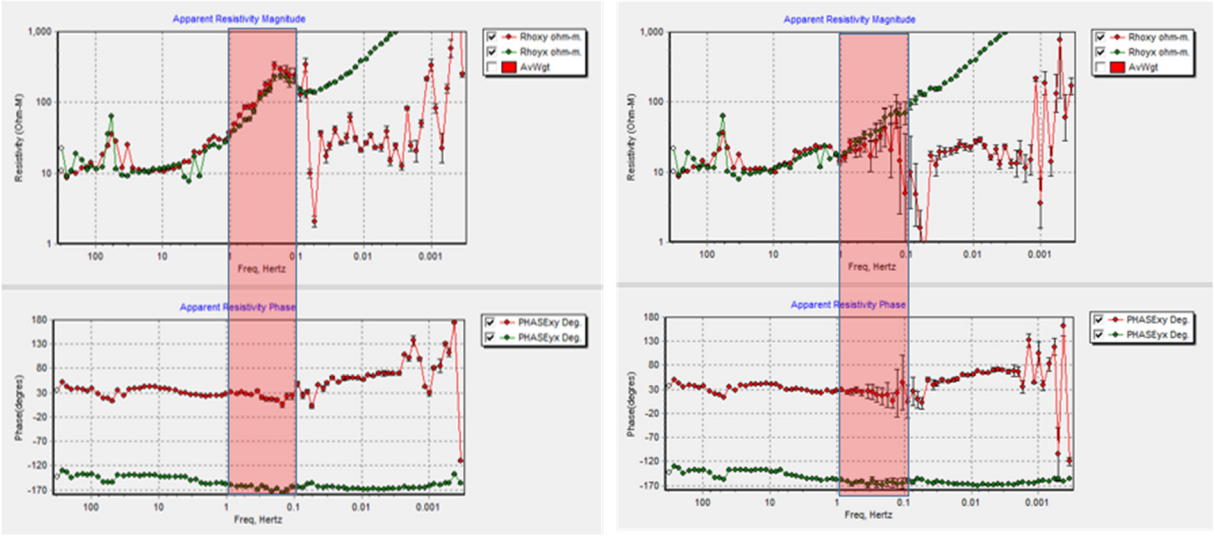

FIGURE 9: Comparison between robust processing (left) and non-robust processing (right) for station MNT-008; in this case the non-robust processing resulted in a "better" apparent curve

3.4 1D data inversion

A one-dimensional (1D) or layered modelling is generally adequate to develop the resistivity anomaly of interest. In order to interpret the data, each sounding was inverted using a special program called TEMTD (Árnason, 2006). The program was used to invert the MT apparent resistivity and phase derived from the rotationally invariant determinant of the MT tensor elements. In the inversion scheme, the layer's thicknesses are kept fixed, equally spaced on log scale (Occam inversion) and the conductivity distribution is forced to be smooth by adjusting the damping parameters. The programme can do 1D inversion for TEM and MT separately or jointly (using both data sets). It can invert either for phase or apparent resistivity of MT data, or both.

The procedure starts from converting the output in .edi format, from the MT Editor to a readable standard .EDI format that the TEMTD program in the Linux operating system environment can read. This is done by using the *spect2edi* script.

All the data were inverted using Occam inversion to create a final model by using several parameters:

1) Factor to scale large uncertainties (-f) which scales down all error bars;
2) Minimum percentage uncertainty (-g) which puts a minimum uncertainty (%) on all data points;
3) Damping parameters which damp differences of resistivity values between layers (R); and
4) Damping parameters which damp the oscillation of resistivity values in the model (S).

All iterations (n) were set to a range of 100 except for the additional re-runs of the generated model. The initial constant resistivity (C) for the automatic model generation started with a low-resistivity value, representing and approximating nearby sea water bodies. Other parameters include H which determines the bottom of the half space, N number of layers, D for the thickness of the top layer, and u and t, where you can omit some data points (Árnason and Benediktsdóttir, 2018).

Figure 10 shows an example of a best fitted model, where the apparent resistivity and phase were inverted for. The blue squares represent the apparent resistivity while the blue circles are the apparent phase, both are derived from the determinant of MT impedance tensor (the light blue squares and circles are data points not used in the inversion). The green graph to the right represents the 1D inversion model and to the left is the model's MT apparent resistivity and phase response both in green. The value below

the station name is the χ -square which is the misfit between the measured and calculated values, normalized by the data uncertainty. "*Shift =1*" denotes the value of the static shift, which is the default static shift value since no TEM data exist. All the 1D models can be seen in Appendix II in Sayco (2018).

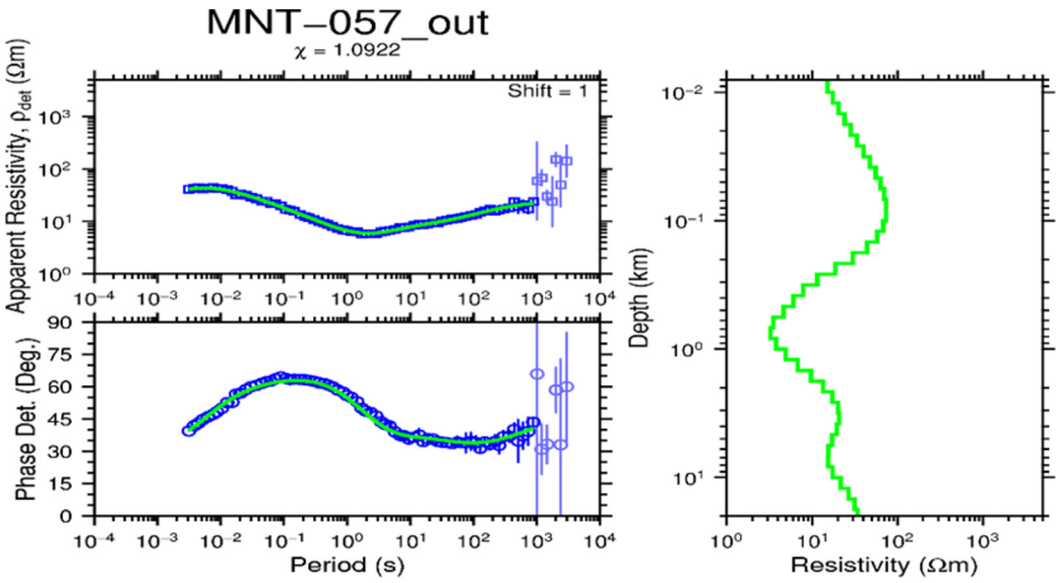

FIGURE 10: Result of 1D inversion of MT data from station MNT-057; blue squares are the MT apparent resistivity and blue circles are MT apparent phase, green graph on right represents the inversion model, and on left is seen the model's MT apparent resistivity and phase responses

Static shift corrections were not taken into consideration since there were no available TEM data in the project area. Instead, a default shift factor of 1 was used for most of the MT stations with no direct effect in cross-section and horizontal slices.

A few soundings caused, the otherwise horizontally continuous resistivity layers, to appear discontinuous. These stations were given a static shift multiplier to ensure the continuity of the horizontally resistivity layers. Figure 11 shows a cross-section from Profile 3, where a couple of MT soundings were corrected for static shift. In this figure, MNT-062 and MNT-034 on profile 3X show a discontinuity at shallow depth, which is suspected to be shifted, particularly at station MNT-034 which

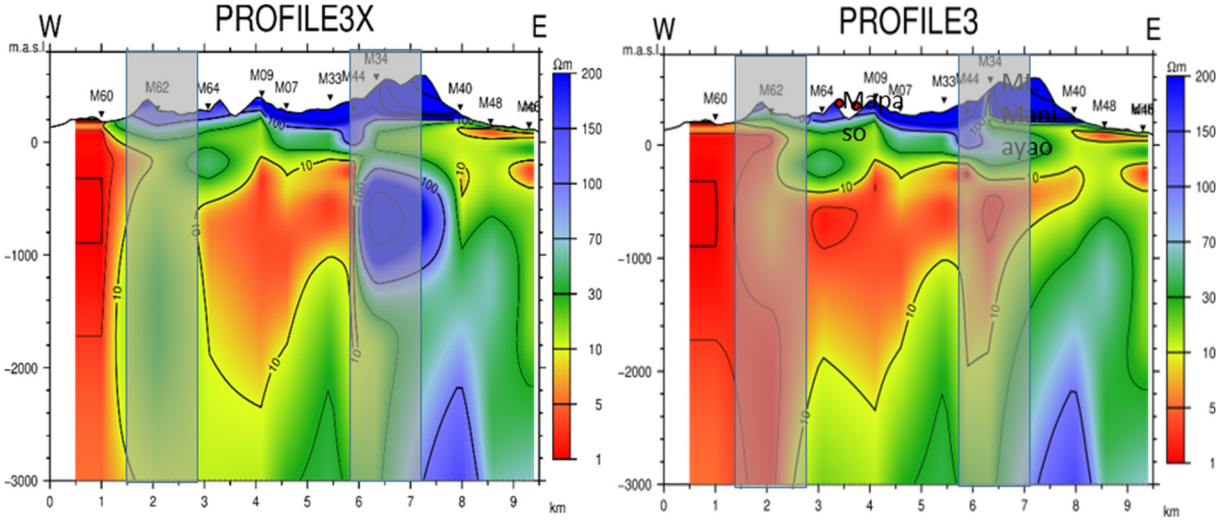

FIGURE 11: Profile 3 corrected for static shift; left side shows MNT-062 and MNT-034 without static shift correction and right side corrected for static shift

gives a high-resistivity value. Stations located in the vicinity of steep topography often suffer from the static shift problem, as well as stations located near shallow lying conductive anomalies (Árnason, 2015). This figure clearly demonstrate that static shift should be given a significant importance to avoid incorrect results.

4. DISCUSSION AND RESULTS

4.1 Geological background of Mainit geothermal project

A total of 50 MT soundings were 1D inverted, within the Mainit geothermal project which is located within the Paco-Maniayao volcanic complex (PMVC) (Figure 12). The PMVC is the youngest

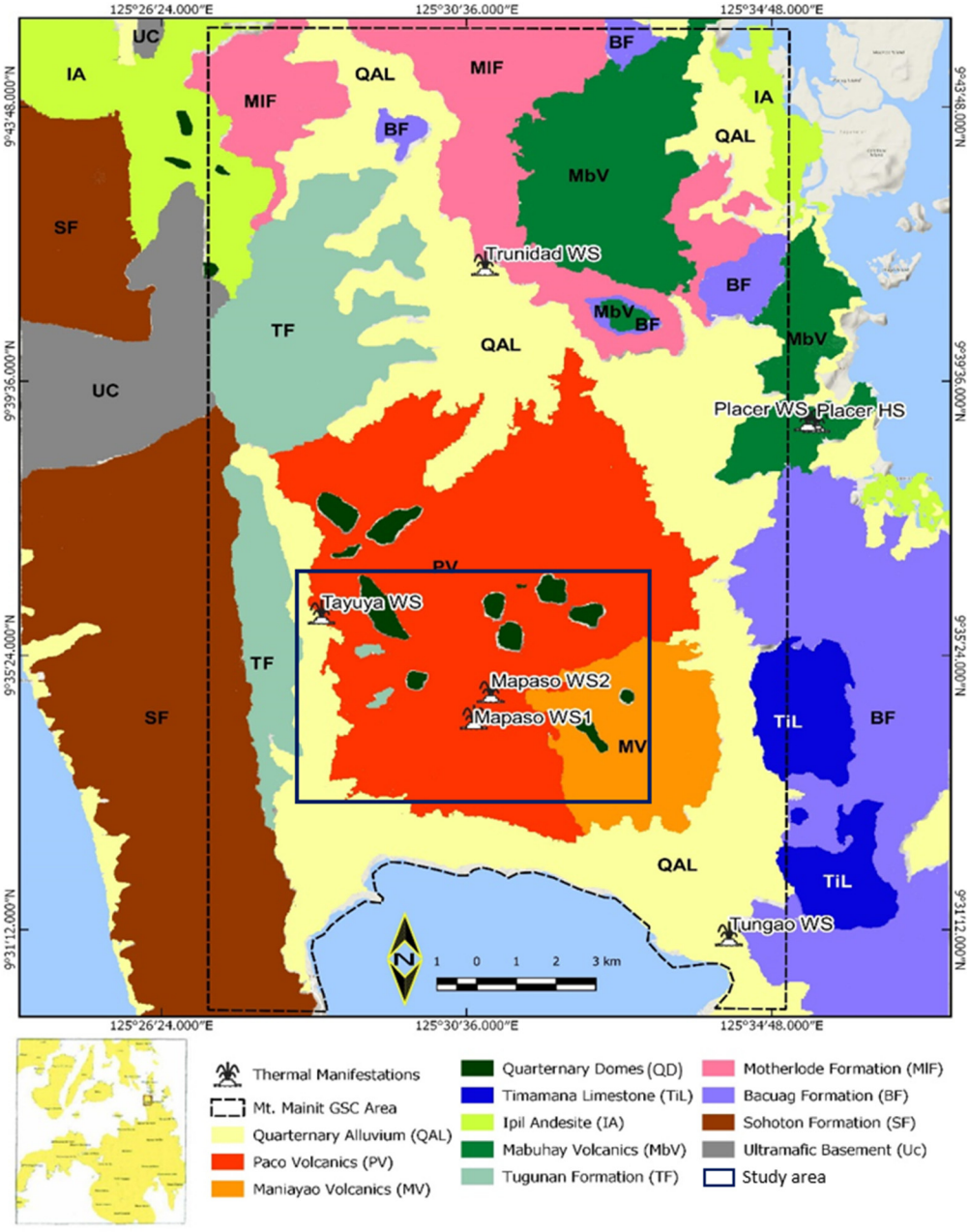

FIGURE 12: Geological map of Mainit geothermal project; the study area is outlined in the small rectangle within the PMVC (adapted from Fermin and Omac, 2012)

formational unit subsequently recognized during the surface geological mapping conducted in the area. The formation is generally andesitic in composition which includes andesites, andesite lava flows, tuff and pyroclastics. Within the PMVC, ancient and young calderas were delineated as well as domes, hills and volcanic centres in the area (Abecia et al., 2013).

Other significant formations mapped within the PMVC are the Tugunan formations and Mabuhay volcanics. They occur in patches over the western and central lowlands (Fermin and Omac, 2012).

4.2 Resistivity cross-sections

The result from the 1D inversion of each sounding can be used to make vertical resistivity cross-sections and depth slices through interpolation between stations (vertical and horizontal). Three E-W cross-sections were made. Their locations are shown in Figure 13 and in Appendix III in Sayco (2018). The profile lines are discussed below and displayed in Appendix IV in Sayco (2018).

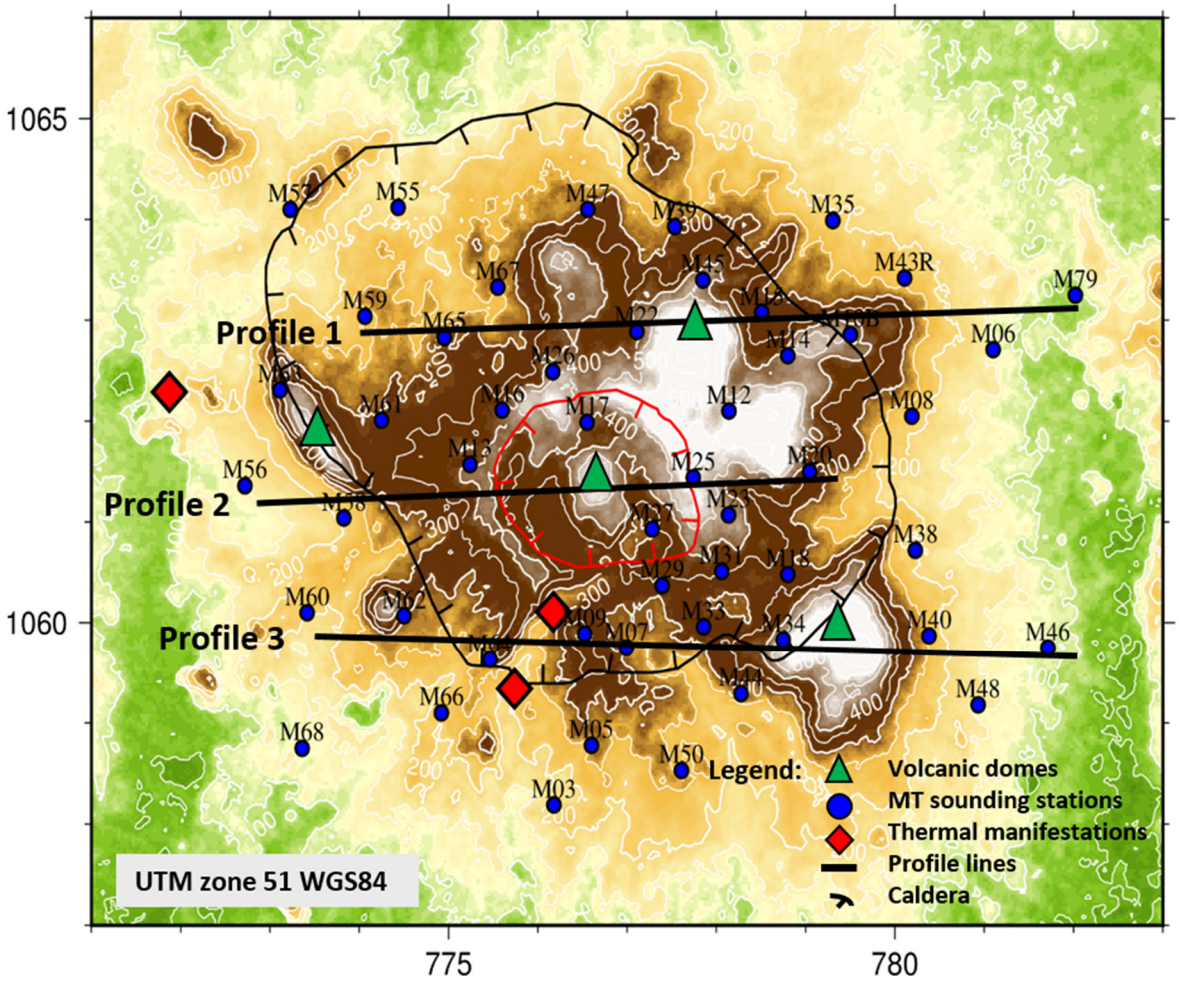

FIGURE 13: MT location map in the Mainit geothermal area showing three resistivity cross-sections in black lines

Profile 1 (Figure 14), which is approximately 8 km long, passes through the central region of Mt. Silop. A shallow resistive layer of about 30-200 Ωm is seen in the central part of the area. It is mostly visible around Mt. Silop and it is thinning out to both sides. At least 3 km thick low-resistivity layer of <20 Ωm in the west is also observed. A conductive layer is seen to thin out to east, where it reaches the surface. A large resistive layer, 30-100 Ωm, is also present in the lower part of the central and eastern part of the section.

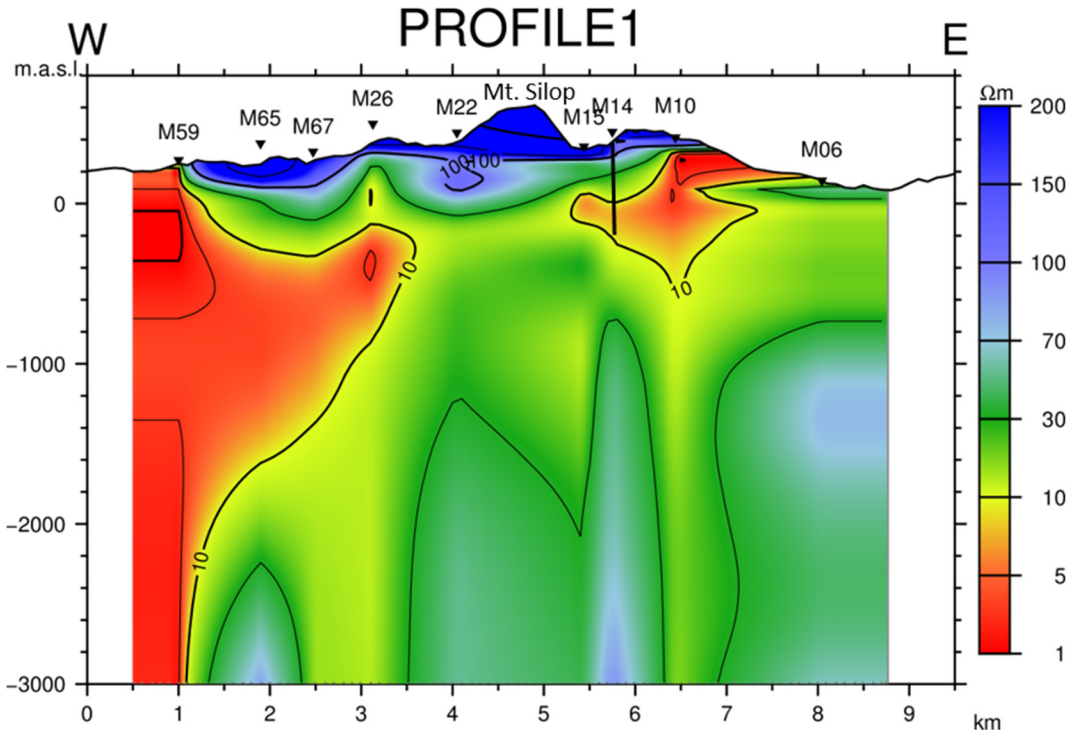

FIGURE 14: Profile 1 lying W-E covering Mt. Silop, location of drill hole from PMC is also shown; location of the profile is given in Figure 13

The location of the drill hole was acquired from the Philex Mining Corporation's technical report in 2011 and it intersects the resistive layer in the model. Figure 15 shows the correlation between the different lithologies belonging to the PMVC well, and the resistivity structures. It shows andesite porphyritic and Tugunan conglomerates overlapping a resistive layer of >10 Ωm, while diorites and basalts coincide with the low-resistivity layer of <10 Ωm. The Bayugo mineral district of PMVC has some identified hydrothermal alteration patterns, like illite-smectite clays (Oliveros, 2011).

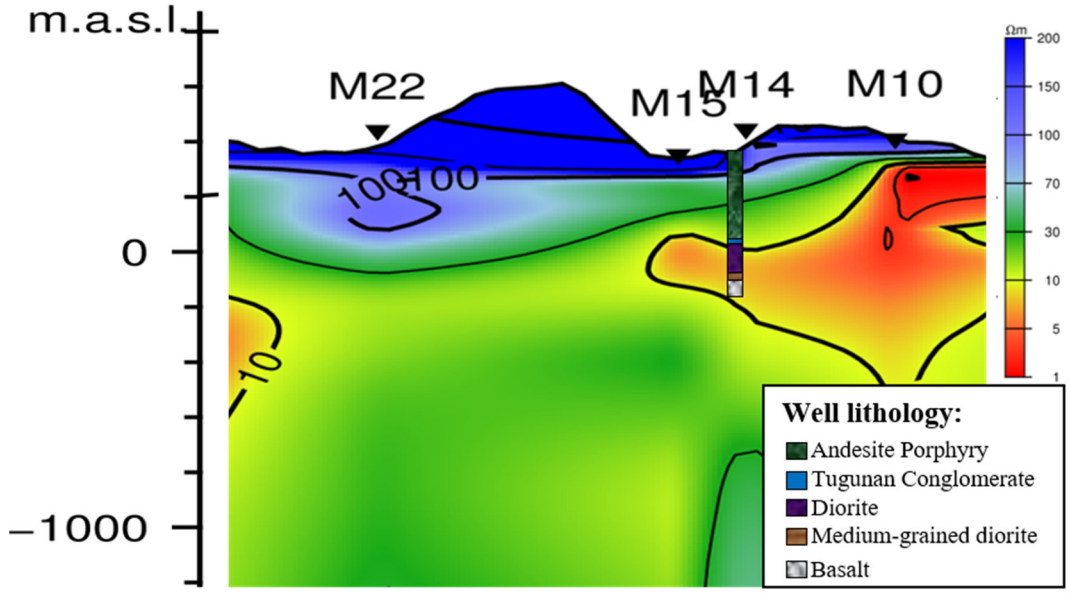

FIGURE 15: Profile 1 trending W-E overlain with lithological data from the PMC drill hole

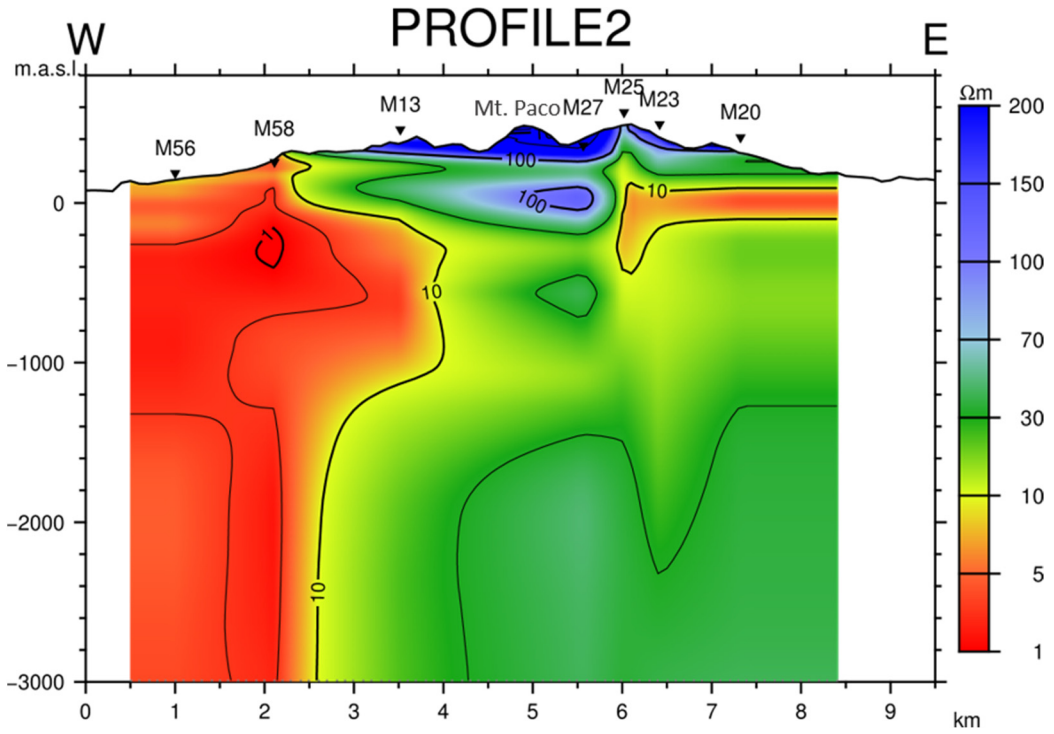

FIGURE 16: Profile 2 trending W-E, covering Mt. Paco

Profile 2 (Figure 16) traverses along Mt. Paco with a length of 8 km. A thick, low-resistivity zone of <5 Ωm is observed in the western area. In the eastern area a thin and shallow lying low-resistivity anomaly extending to the east is observed. A resistive region of 30-100 Ωm is also observed just below Mt. Paco. A thin superficial resistive layer of 30-200 Ωm is observed around Mt. Paco.

Profile 3 (Figure 17) cuts across the Mapaso thermal springs and a portion of Mt. Maniayao in the east. It covers a length of around 9 km. A shallow high-resistivity layer of 30-200 Ωm covers the central

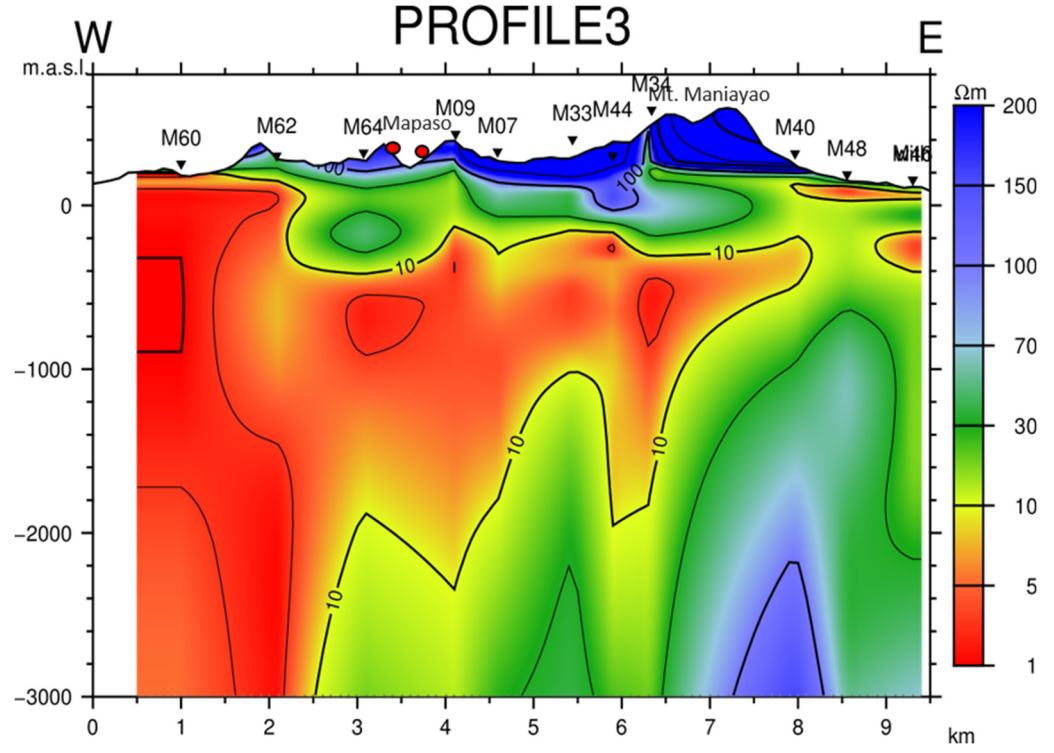

FIGURE 17: Profile 3 trending W-E, covering Mt. Maniayao and Mapaso hot springs

region of the area. Underneath, at 200 m depth below sea level, there is a low-resistivity layer which extends from a thick low-resistivity zone of <10 Ωm in the east, across the section to the west, where it reaches the surface as well as deeper levels. A high-resistivity layer of 40-100 Ωm in the eastern part is prominent underneath the low-resistivity layer.

4.3 Resistivity maps

Horizontal maps at different elevations were generated and are discussed below. Additional maps are published in Appendix V in Sayco (2018).

Figure 18 shows the resistivity at 200 m a.s.l. Areas with high-resistivity values ranging between 70 and 200 Ωm are seen in the northwest and southeast regions surrounding the volcanic domes. A small region with lower resistivity, around 5-10 Ωm, is seen to the west just beside Mt. Masapilid. Another small, conductive area with resistivities of 5-25 Ωm is observed to the east of Mt. Silop.

Figure 19 shows the resistivity at sea level. Three distinct regions of high-resistivity values in the range 15-100 Ωm are seen east of Mt. Masapilid and within Mt. Maniayao. The high-resistivity block to the northeast of Mt. Silop is the most distinct and extends further to the east. Low resistivity, < 10 Ωm, is observed both in the west and in the southernmost part.

Figure 20 shows the resistivity structure at 500 m below sea level. An extensive low-resistivity body, <10 Ωm is seen, covering the western region with a small patch of higher resistivity, 15 Ωm, seen near Mt. Masapilid. On the other hand, relatively high resistivity values, ranging from 25 to 70 Ωm, are present in the eastern region.
F

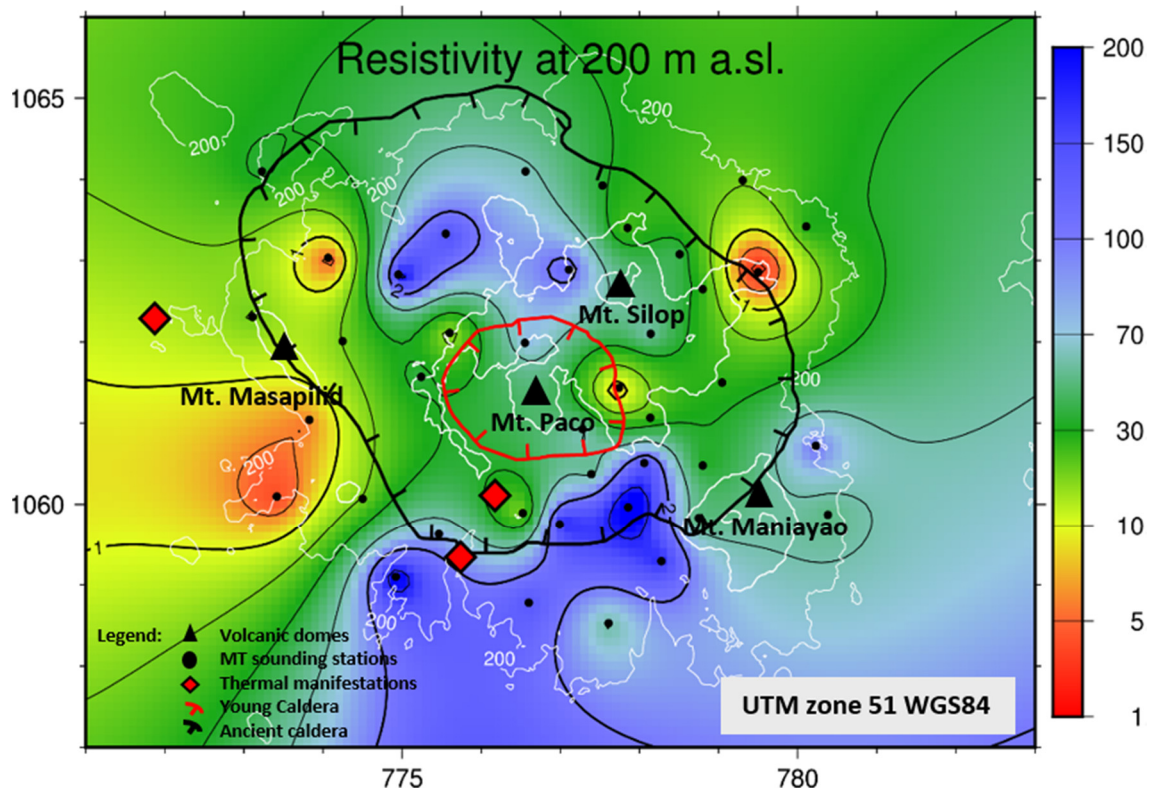

FIGURE 18: Resistivity in Ωm, at 200 m a.s.l.

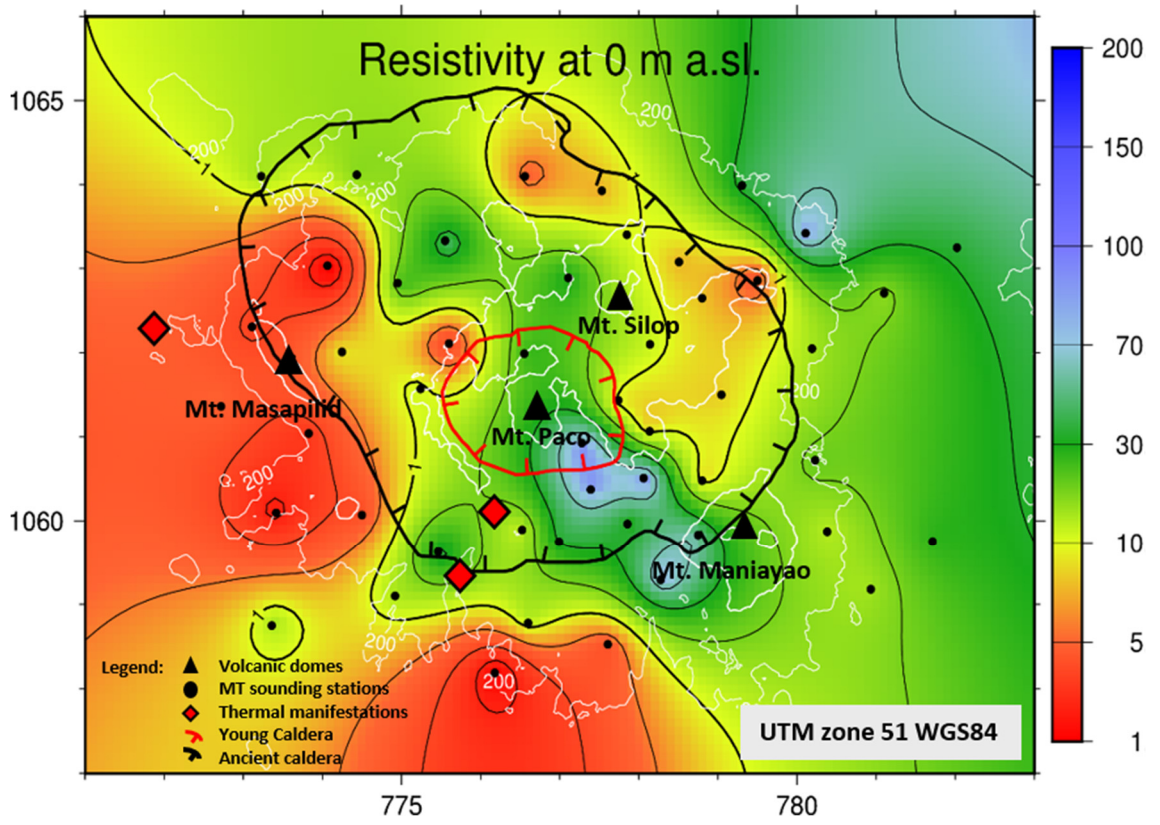

FIGURE 19: Resistivity in Ωm, at sea level

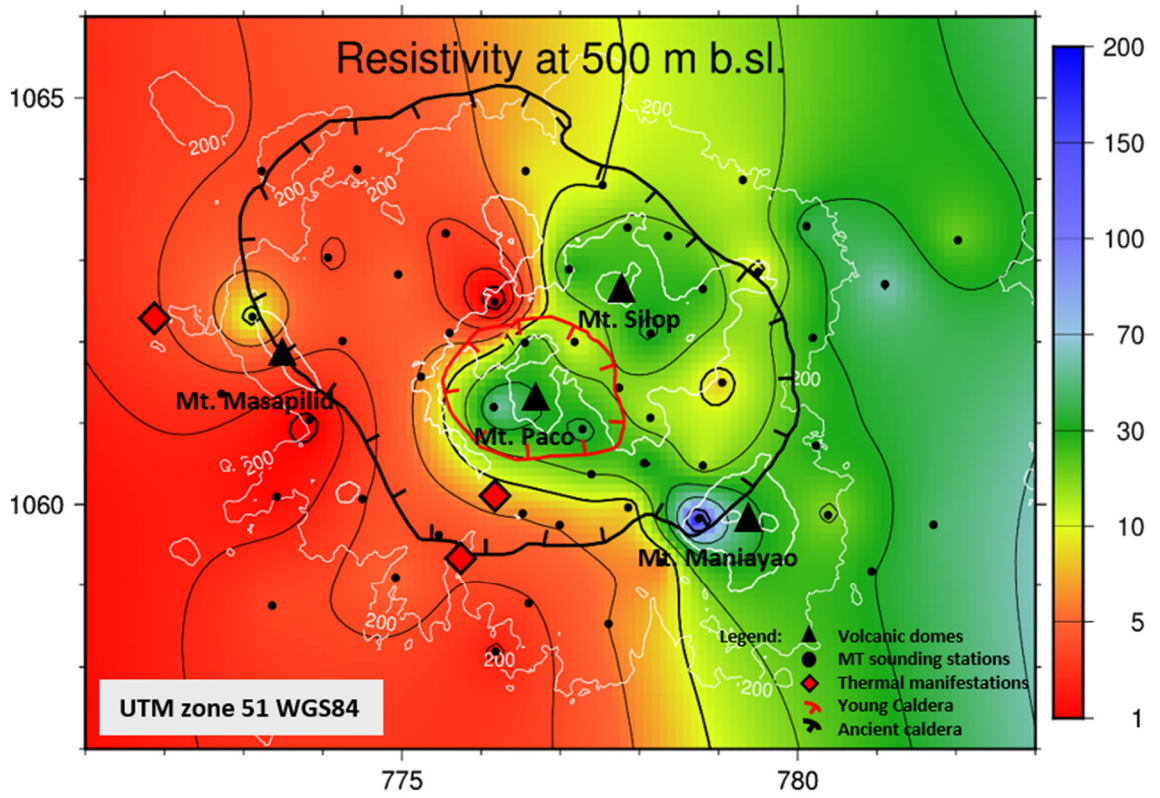

FIGURE 20: Resistivity at 500 m b.s.l.

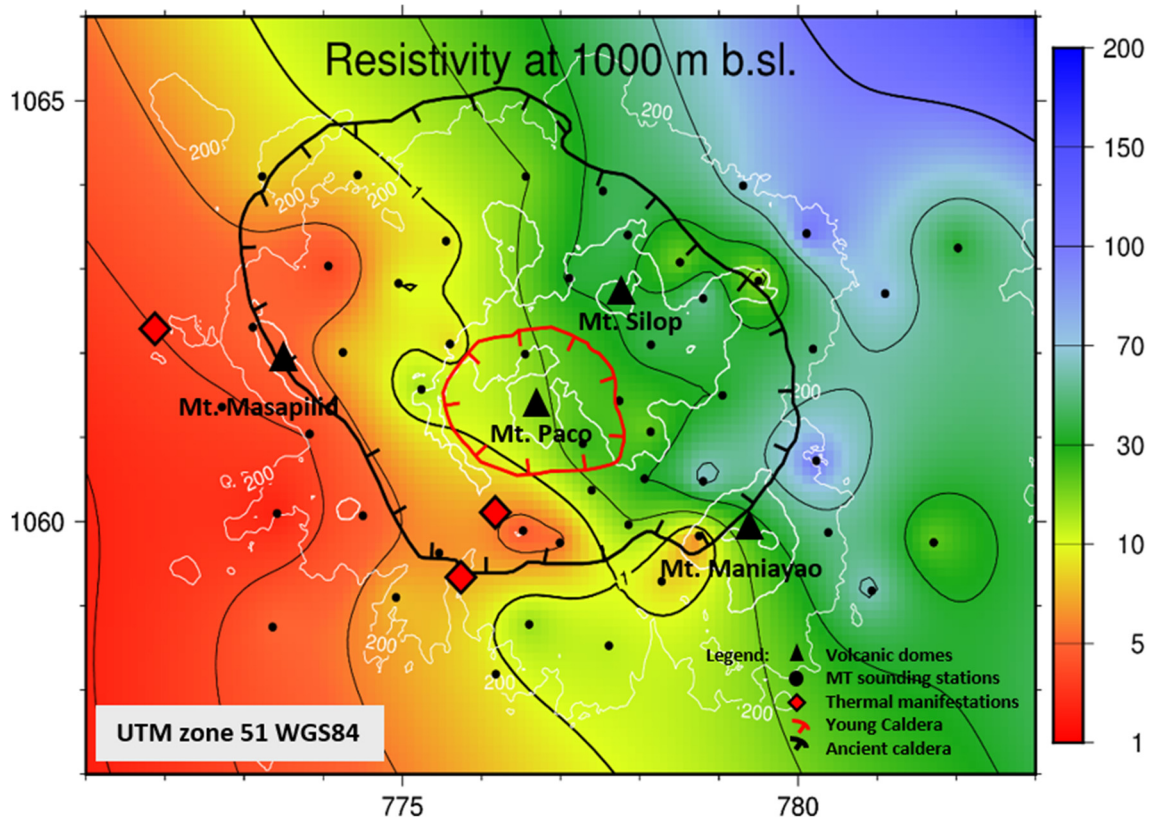

FIGURE 21: Resistivity at 1000 m b.s.l.

Figure 21 shows the resistivity at 1 km below sea level. Here, a lateral contrast of low resistivity, < 20 Ωm, in the west and higher resistivity of 20-100 Ωm in the east is seen. This lateral boundary coincides well with the eastern volcanic domes of Mt. Silop and Mt. Maniayao.

4.4 Strike analysis

Lateral resistivity contrasts are reflected in electrical strike analysis. These can be faults and fractures not necessarily seen at the surface. Rose diagrams, based on the Tipper strike were obtained for different periods as shown in Appendix VI in Sayco (2018). Figure 22, shows the Tipper strike for periods in the range of 1-10 s where a lateral resistivity contrast trending NNE-SSW was observed. Induction arrows at 1 s period are also displayed, where the blue arrow, representing the real part of the induction arrows, is pointing away from the conductive body, indicating that a low-resistivity layer is present in the area. This is consistent with the resistivity structure shown in Figures 18-21. Induction arrows at different periods can be seen in Appendix VII in Sayco (2018).

At a greater depth for periods in the range of 10-100 s, the Tipper strike starts to align parallel with the conductive sea located near the western side of the area, as shown in Figure 23. The ocean is also well represented by the induction arrows at 50 s where the real parts (blue arrows) point to the east, away from the highly conductive body (the sea). When MT data are obtained in the vicinity of the coast, the surrounding sea makes it difficult to interpret the subsurface structures, especially the deeper parts. Therefore, correction methods should be applied to enhance the inversion results and to recover the true response of the subsurface in the MT data (Yang et al., 2010).

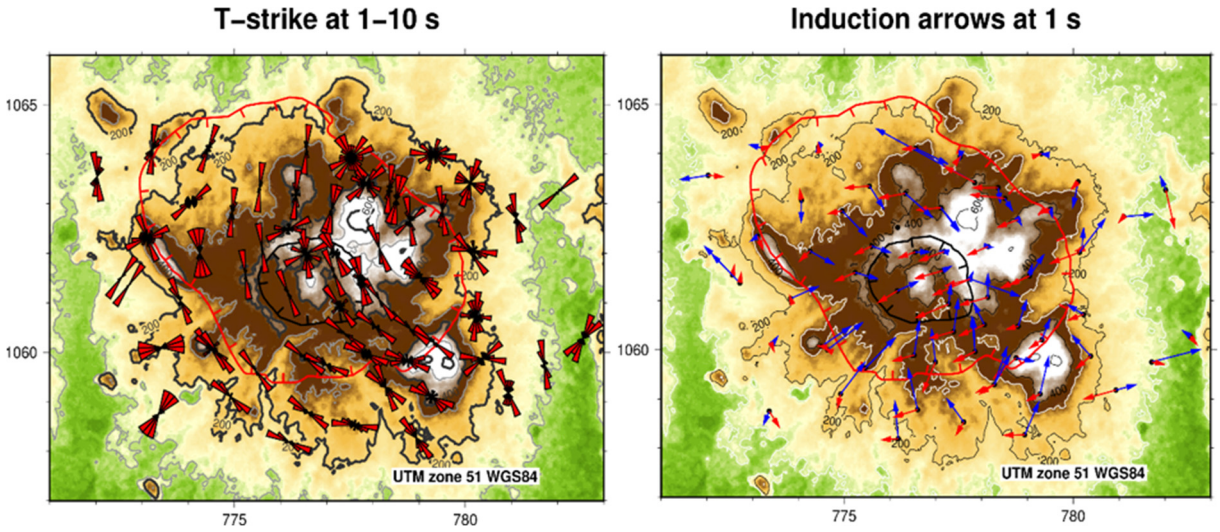

FIGURE 22: Tipper strike for periods between 1 and 10 s (left) and induction arrows at period 1 s (right); blue and red arrows are the real and imaginary parts, respectively

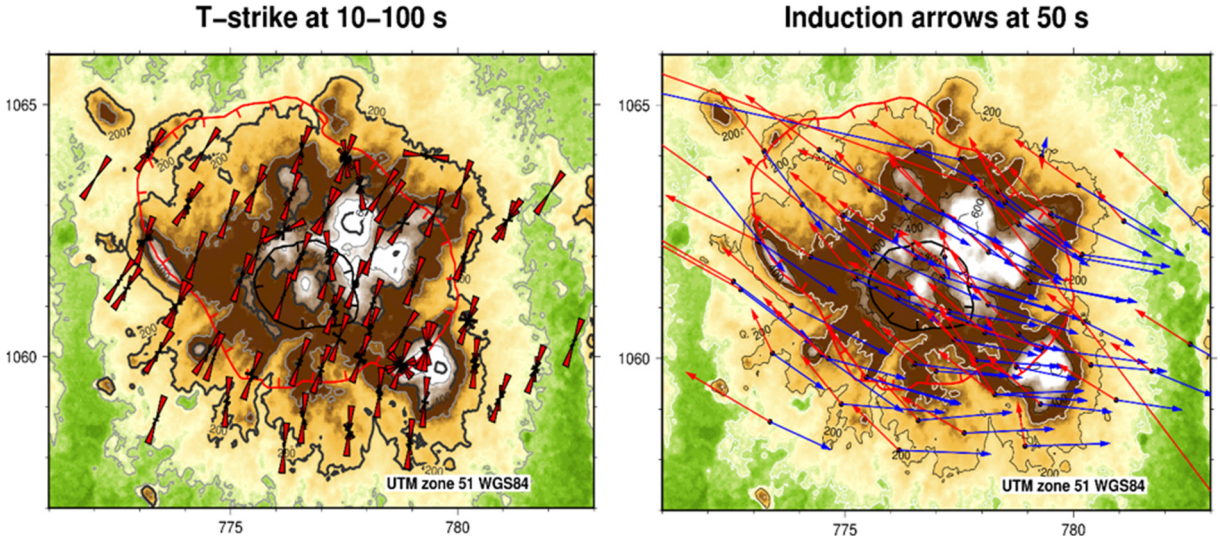

FIGURE 23: Tipper strike for periods between 10 and 100 s (left) and induction arrows at period 50 s (right); blue and red arrows are the real and imaginary part, respectively

4.5 Data interpretation

The presence of high-resistivity values within the cluster of volcanic domes and hills in the Paco-Maniayao volcanic complex as observed in the resistivity structure at 200 m above sea level (Figure 18) is interpreted to be the youngest rock unit in the area, composed mostly of andesites (Fermin and Omac, 2012). This was confirmed by the presence of an andesite porphyritic cover within the Boyongan and Bayugo area (Oliveros, 2011) as intersected by Profile 1. The thick low resistivity in the western region that extends to a depth of 3 km, as shown in Figures 14-17, is believed to be part of the Tugunan sedimentary formation which consists of sandstone, siltstone and general clay deposits. In addition, the fresh water from Lake Mainit, penetrating the more permeable layers of siltstone and sandstone of the Tugunan sediments, may also influence the extent and depth of the conductive layer (Abecia et al., 2013).

Higher resistivity values, >40 Ωm, which are believed to associated with the intrusive bodies of the older Mabuhay volcanics, are seen beneath the thinner conductive layer in the eastern part of the profiles. Lateral contrasts between the high-resistivity region to the east and low-resistivity body to the west are clearly observed in the resistivity map at 1 km below sea level. Possible faults inferred by MT might be the reason for this major discontinuity between the low-resistivity zone of the Tugunan sedimentary layer and the high-resistive layer of the intrusive blocks (Africa et al., 2015).

The data from the drill holes of PMC at Bayugo mineral district (Figure 15) suggest the presence of geothermal fluid as indicated by the scattered alteration, like illite-smectite (Oliveros, 2011). However, taking into account the presence of copper-gold deposits found in the Boyongan and Bayugo mineral district (Rohrlach, 2005), the low-resistivity layer observed near the surface and the continuous high-resistivity layer observed from top to bottom in the eastern section of Profile 1, suggests a relatively old and waning geothermal system (Abecia et al., 2013). This supports the distribution of relatively hotter springs in Placer and Tungao which are found within the high-resistivity intrusive block in the eastern zone, compared to the thermal springs in the western region which are found within the low-resistivity/sedimentary region despite their proximity to the young volcanic domes.

5. CONCLUSIONS AND RECOMMENDATIONS

MT data from the Mainit geothermal project were reprocessed and 1D inverted. The results are comparable with previous studies. Static shift correction was not performed since TEM data were not available. However, some stations were corrected due to resistivity inhomogeneity at shallow depths as clearly seen in the profiles. This shows that static shift should be given due importance and the parameters should be imposed during the inversion process.

Based on the result of the inversion, the high-resistivity layer to the northeast of PMVC is believed to be a relatively old, intrusive body. The intrusive body could be the possible heat source which is also the one responsible for the extensive mineralization in the area, as manifested by mineral deposits. This supports the distribution of relatively warmer springs in the eastern region compared to the thermal manifestations in the western region. However, there is no evidence of a typical resistivity anomaly where up-flow and out-flow can be identified.

To get a more detailed resistivity model, 3D inversion should be performed. With this, the 3D features of the area will be resolved better, both laterally and at depth. It will also account for the effect of the ocean, which is very important in settings such as the one described here.

Finally, it is recommended to collect TEM at the same sites as the MT soundings to correct for the static shift of the MT data.

ACKNOWLEDGEMENTS

First and foremost, I would like to express my sincerest gratitude to the UNU-GTP staff, especially to Mr. Lúdvík S. Georgsson, for the invitation and for making me part of this 6-months training programme. For all the knowledge, guidance and support that you have given to me and to my co-fellows is much appreciated. Special thanks to Mr. Ingimar G. Haraldsson, for coming all the way to the Philippines. Without your presence, I would not be here. Many thanks also to Markús A.G. Wilde, Ms. Thórhildur Ísberg and Ms. Málfrídur Ómarsdóttir, for their patience, facilitation and full support to all our needs. You all made our Icelandic experience truly rewarding and memorable.

To my ever supportive supervisor, Ásdís Benediktsdóttir and the geophysics group of ISOR headed by the very energetic Gylfi Páll Hersir and very dedicated Knútur Árnason, together with the lecturers during the specialized courses, a million thanks to all of you. Your generosities in sharing your knowledge and expertise are truly remarkable and will be treasured.

To my co-fellows, especially the geophysics group, Thank you! I really appreciate all your presence. Cheers to all the good times that we had! Truly an amazing experience. May our friendship blossom even outside this training programme and I'm hoping to see you around.

I would like to acknowledge also my employer, Department of Energy, for granting me a study leave and for giving me the opportunity to undergo this training. To my officemates in GEMD, for their support and assistance especially during the course of this project, Thank you!

Lastly, to my family, relatives, friends and the Filipino community here in Iceland, thank you for keeping me going day by day. For all your encouragements and unending support, Thank you!

Above all, to Almighty God! For all the blessings you showered upon me, the grace and talent you have given to me and for the good health, Thank you.

REFERENCES

Abecia, V.M., Africa, J.R. and Fermin, M.R.D., 2013: *Mainit geothermal prospect integrated resource assessment*. EDC – Energy Development Corporation, Resource Technology Division, Geosciences and Reservoir Engineering Group, unpublished internal report.

Africa, J. R., Monasterial, J.L.C., Layugan, D.B., Rigor, D.M., Los Baños, E.F., 2015: Magnetotellurics (MT) resistivity signature of a geothermal prospect with Au-Cu mineralization in Surigao del Norte, Philippines. *Proceedings of the World Geothermal Congress 2015, Melbourne, Australia*, 6 pp.

Africa, J.R., 2018: *Fundamentals on MT method.* Department of Energy, Philippines, unpublished lecture material.

Árnason, K., 2006: *TEMTD, a program for 1D inversion of central-loop TEM and MT data. Short manual*. ÍSOR – Iceland GeoSurvey, Reykjavík, Iceland, internal report, 17 pp.

Árnason, K., 2015: The static shift problem in MT soundings. *Proceedings of the World Geothermal Congress 2015, Melbourne, Australia*, 12 pp.

Árnason, K. and Benediktsdóttir, Á, 2018: *TEMTD, a program for separate or joint 1D inversion of TEM and MT data*. UNU-GTP, Iceland, unpublished lecture material.

Árnason, K., Karlsdóttir, R., Eysteinsson, H., Flóvenz, Ó.G., and Gudlaugsson, S.Th., 2000: The resistivity structure of high-temperature geothermal systems in Iceland. *Proceedings of the World Geothermal Congress 2000*, *Kyushu-Tohoku, Japan,* 923-928.

Catane, J.P.L., Herras, E.B. and Maneja, F.C., 1989: *Geoelectric investigation in the Surigao geothermal prospect, Mainit, Surigao del Norte*. PNOC-EDC, Philippines, report.

Christopherson, K.R., 1998: MT gauges earth's electric fields, geophysical corner. *AAPG Explorer, 1998,* 22-25.

DOE, 2010: *Geothermal service contract area of the Mainit geothermal project.* Department of Energy, Philippines, map.

Fermin, M.D. and Omac, X.L., 2012: *Preliminary geological assessment of the Mainit geothermal prospect*. EDC – Energy Development Corporation, unpublished internal report.

Flóvenz, Ó.G., Hersir, G.P., Saemundsson, K., Ármannsson, H., and Fridriksson Th., 2012: Geothermal energy exploration techniques. In: Sayigh, A. (ed.), *Comprehensive renewable energy, vol 7*. Elsevier Oxford, United Kingdom, 51-95.

Flóvenz, Ó.G., Spangerberg, E., Kulenkampff, J., Árnason, K., Karlsdóttir, R., Huenges, E., 2005: The role of electrical interface conduction in geothermal exploration. *Proceeding of the World Geothermal Congress 2005, Antalya, Turkey,* 9 pp.

Georgsson, L.S., 2013: Geophysical methods used in geothermal exploration. *Presented at "Short Course VIII on Exploration for Geothermal Resources", UNU-GTP, KenGen and GDC, Lake Naivasha, Kenya,* 22 pp.

Hermance, J.F., 1973: Processing of magnetotelluric data. *Physics of the Earth & Planetary Interiors, 7,* 349-364.

Hersir, G.P., and Björnsson, A., 1991: *Geophysical exploration for geothermal resources. Principles and applications*. UNU-GTP, Iceland, report 15, 94 pp.

Jones, A.G., 1988: Static shift of magnetotelluric data and its removal in a sedimentary basin environment. *Geophysics, 53-7*, 967-978.

Kearey, P., Brooks, M. and Hill, I., 2002: *An introduction to geophysical exploration* (3rd ed.). Blackwell Scientific Publ., London, 272 pp.

Oliveros, N.C., 2011: *Technical report on the Bayongan-Bayugo deposit in Surigao del Norte, Mindanao, Philippines.* Philex Mining Corporation, Technical report of Exploration results and mineral resources.

Panem, C.C., 1975: *The geology of the Surigao geothermal field*. *The ComVol Letter, IX.*

Phoenix Geophysics, 2005*: V5 system 2000 MTU/MTU-A data processing – A user guide*. Phoenix Geophysics, Ltd., Toronto. Press Ltd., Oxford, 527 pp.

Pinto, V., Fontes, S.L. and Ulugergerli, U., 2011: A discussion about robust and classical magnetotelluric processing technique: A case study on Santos basin. *Proceedings of the 12th International Congress of Brazilian Geophysical Society, Rio de Janeiro.*

Rohrlach, B.D., 2005: *Independent geological report on the Surigao property group Northern Mindanao, Philippines.* MRL Gold Philippines, Inc. and Panoro Minerals Ltd., report.

Sanchez, D., 1989: *Geochemical assessment of Surigao geothermal prospect*. PNOC-EDC, Metro Manila, Philippines, report.

Sayco, J.G., 2018: *Appendices to the report: 1D inversion of magnetotelluric data from Mainit geothermal area, Philippines*. UNU-GTP, Iceland, report 25, appendices, 89 pp.

Tebar, H.J. and Pagada, E.S., 1990: *Geoscientific evaluation of the Surigao geothermal prospect, northwest Mindanao (compilation)*. PNOC-EDC, Exploration Section, report.

Vozoff, K., 1990: Magnetotellurics: principles and practices. *Proceedings of the Indian Academy of Science-earth and Planetary Sciences*, *99*, 441-471.

Wikipedia, 2018: *Map of NE-Mindanao, Philippines.* Wikipedia.

Yang, J., Dong-Joo Min and Hai-Soo Yoo, 2010: Sea effect correction in magnetotelluric (MT) data and its application to MT soundings carried out in Jeju Island, Korea. *Geophysical J. International*, *182-2,* 727-740.